Simple and Flexible Power Loss Minimizer with Low-Cost MCU Implementation for High-Efficiency Three-Phase Induction Motor Drives

Adriana Bruno, Massimo Caruso, Antonino O. Di Tommaso, Rosario Miceli, Claudio Nevoloso and Fabio Viola
Department of Engineering - University of Palermo, Viale delle Scienze, Building nr. 9, 90128 Palermo, Italy.
e-mail: antoninooscar.ditommaso@unipa.it

***Abstract*—This paper presents a simple, practical and low-cost implementation of a power losses minimization algorithm for three-phase induction motors taking also into account both iron core losses and magnetic saturation. The algorithm evaluates, in real-time, the optimal direct axis magnetizing flux component for efficiency enhancement of the drive. A further advantage of the proposed technique is represented by a flexible and low-cost implementation by means of an ATMEL ATSAM3X8E microcontroller. The power loss minimization algorithm is tested preliminarily by means of several simulations, then, experimentally validated by applying the proposed control strategy on a 5.5 kW Field Oriented Control (FOC) induction motor drive. Significant results in terms of efficiency enhancement are presented and discussed, demonstrating that the proposed online control can significantly decrease the power losses of the drive.**

***Index Terms*—Loss Model Control, Field Oriented Control, power losses minimization, induction motor.**

I. Introduction

Over the last decades, the research in the field of electric drives has directed the efforts towards the conception of innovative control techniques, capable of enhancing the performance of electric motors. Nowadays, the Induction Motor (IM) is adopted in a very wide range of applications because of its high flexibility and robustness. With regard to this typology of electric machine, recent literature proposes several control techniques, whose performances are strictly influenced by the range of speed, the load conditions and the area of application. The literature proposes several online control strategies that set the condition of maximum efficiency during the operation of the motor by using feedback signals and information derived from the motor itself, consequentially adapting the parameters of the controller. Generally, these strategies, aimed to enhance the efficiency of IM, can be classified into three main categories [1], [2]:

1) *Loss Model Control* (LMC), which takes into account a specific model of the machine and minimizes the power losses by acting on the magnetization level of the machine [3]–[17].
2) *Search Control* (SC), consisting on a real-time detection of the minimum input power by iteratively changing the magnetization level of the machine for a given working condition in terms of load and speed [18]–[22].
3) *Hybrid Control* (HC), which combines the two previously mentioned techniques [23]–[25].

The Loss Model Control searches the maximum efficiency for any working point in terms of load and speed by taking into account the mathematical model of the motor. Normally, this model includes copper and iron losses and it depends on both the electrical and mechanical IM parameters [10], such as stator and rotor resistances, magnetizing reactance and iron core equivalent resistance. Therefore, the accuracy of this technique strictly depends on the accuracy with which the IM parameters are known. These parameters could be pre-determined through several tests (no-load, locked rotor, etc.) and assumed as constant values in the applied control algorithm [10]–[12]. However, this method does not ensure a high accuracy on the power loss identification, due to the wide variation of these parameters with temperature, frequency and current amplitude [26]. As an alternative, the parameters can be determined via offline look-up tables, which leads to very complex computations [27]. Another possibility consists on their online estimation for a more accurate loss model. For instance, Kioskeridis [12] and Aguilar [28] proposed a self-tuning online estimation for the rotor resistance and the magnetizing inductance of the IM. The work in [26] modifies the IM parameters through polynomial functions according to a dynamic identification property of the motor, such as temperature, load torque and inertia. The estimation of the IM parameters could be also provided through genetic algorithms, as shown in [29]. Some of the LMCs do not consider the leakage inductance in order to simplify the equivalent circuit of the IM [4], [10].

Besides the accuracy of the loss model taken into account, several control strategies for the power loss minimization are proposed in literature. For example, Lorenz et al. [30] considered objective functions for the online determination of the optimal flux trajectories for the power losses minimization. Uddin et al. [11] proposed a power loss minimization technique by acting on the magnetizing current from a steady-state IM model, taking into consideration both copper and iron losses. In [10], the loss minimization is achieved by the adequate energy balance between copper and iron losses, obtaining also a good dynamic response. Yuying et al. adopted dynamic programming in order to determine the loss-minimizing stator flux trajectory for unknown load profiles [31]. Qu et al. [16] proposed a dynamic space-vector model for power losses minimization, providing a method for determining the optimal reference flux at each sampling

period. Swarm Intelligence (SI) has also been adopted for the efficiency enhancement of electric drives [32].

Generally, the variable for the power loss minimization is the magnetizing current. However, many works considered other loss variables: for instance, Mannan et al. [33] proposed a control of the slip frequency in order to minimize the power losses of an IM controlled with a traditional Field Oriented Control (FOC). A linearized steady-state model that considers the slip speed as a loss variable was presented in [13], [14]. Other studies have proposed either magnetizing flux [12], [16] or stator currents [11] as loss variables.

The second category of the online LMTs (Loss Minimization Techniques) is represented by the Search Control, which has been widely applied by many researchers [21], [22], [27], [34]. One of the main drawbacks of this technique is represented by the fact that it does not reach a pure steady-state condition and this causes oscillations in the air-gap flux, leading to undesirable torque ripples and speed fluctuations. Moreover, the system converges to the optimal point with a significant time delay, detecting also oscillations around the optimal value of the magnetizing flux value [19].

Finally, the third control strategy is the Hybrid Control, consisting on a combination of LMC and SC and aimed at exploiting the advantages of both approaches, avoiding at the same time their major drawbacks. For instance, Vukosavic and Levi [23] presented a hybrid solution between LMC and SC with very fast convergence, in which the minimum power loss condition is obtained from a functional approximation of the motor and the power converter losses.

In this context, this work proposes an enhanced but simple procedure for power losses minimization that adopts the magnetizing flux as the loss variable and takes into account both the iron core losses and the magnetic saturation effects, in order to consider the non-linear phenomena involved during the working operation of the machine. A significant efficiency enhancement is achieved for any condition in terms of load and speed during the actual operation of the IM. The easy, flexible and low-cost implementation of the control system is achieved by means of an ATMEL ATSAM3X8E microcontroller, which represents another advantage of the proposed control technique. Therefore, the main features of the proposed technique can be summarized in: simplicity, due to the easiness of its real-time implementation due to the use of simple algebraic equations, flexibility, due to the possibility of adapting the power loss minimizer for any working condition of any IM type, good accuracy, due to the highly accurate model taken into account that considers the variability of the IM parameters, and, finally, low-cost implementation, provided by the adoption of the ATMEL microcontroller. The control strategy is firstly implemented in the Simulink environment and then experimentally validated and compared with the traditional FOC strategy on a 5.5 kW IM. The results demonstrate that this algorithm is suitable for a specific range of working conditions, providing interesting energy savings.

More in detail, this work is organized as follows: Section II introduces the proposed algorithm for the power loss minimization. Section III describes the simulation results obtained by means of the Simulink environment. Finally, Section IV reports the test bench equipment and the experimental results carried out for the proposed investigation, highlighting also the technical and economic features of the adopted system.

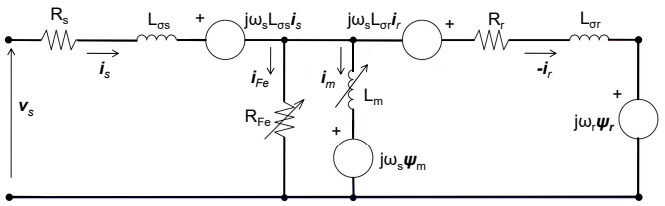

Figure 1. IM equivalent circuit for the LMC identification.

II. Proposed Loss Model Technique

This Section presents the procedure for the power loss minimization proposed by the Authors, which depends both on direct-axis and quadrature-axis magnetizing flux components, namely ψ_{md} and ψ_{mq}. More specifically, the IM dynamic model taken into account, defined in the synchronous $(d-q)$ reference frame, is depicted in Fig. 1.

By imposing the rotor flux oriented control condition

$$\frac{d\psi_{rq}}{dt} = \psi_{rq} = 0, \tag{1}$$

the model is described by the following equations:

$$T_{\sigma r}\frac{d\psi_{rd}}{dt} + \psi_{rd} = \psi_{md}, \tag{2}$$

$$\omega_s = \frac{d\theta_s}{dt} = \frac{T_{\sigma r}}{\psi_{mq}}\psi_{rd} + \omega_r \tag{3}$$

$$T_{\sigma Fe}\frac{d\psi_{md}}{dt} + \psi_{md} = L_{\sigma r}\left(i_{sd} - i_{md}\right) + \psi_{rd} + T_{\sigma Fe}\omega_s\psi_{mq}, \tag{4}$$

$$T_{\sigma Fe}\frac{d\psi_{mq}}{dt} + \psi_{mq} = L_{\sigma r}\left(i_{sq} - i_{mq}\right) - T_{\sigma Fe}\omega_s\psi_{md}, \tag{5}$$

where ψ_{rd} and ψ_{rq} are the direct-axis and quadrature-axis rotor flux components, respectively, ω_r and ω_s represent the rotor speed and the synchronous speed, respectively, θ_s the rotor flux angular position, i_{sd} and i_{sq} are the direct-axis and quadrature-axis stator current components, respectively, L_m is the magnetizing inductance, R_{Fe} is the core loss resistance, R_r and $L_{\sigma r}$ are the rotor resistance and the rotor leakage inductance, respectively, $T_{\sigma r} = {}^{L_{\sigma r}}/_{R_r}$ and $T_{\sigma Fe} = {}^{L_{\sigma r}}/_{R_{Fe}}$ are rotor time constants. The direct-axis and quadrature-axis magnetizing current components, namely i_{md} and i_{mq}, can be determined as

$$i_{md} = i_m\frac{\psi_{md}}{\psi_m} \tag{6}$$

and

$$i_{mq} = i_m\frac{\psi_{mq}}{\psi_m}, \tag{7}$$

where

$$\psi_m = \sqrt{\psi_{md}^2 + \psi_{mq}^2}. \tag{8}$$

If saturation of the magnetic circuit is neglected, the magnetizing current is calculated as $i_m = {}^{\psi_m}/_{L_m}$, otherwise magnetic saturation is taken into account by introducing the IM magnetizing characteristic $i_m = f(\psi_m)$.

From the circuit represented in Fig. 1, the expression of power losses ΔP_{loss} is given by the sum of the stator copper losses, $\Delta P_{Cu,s}$, rotor copper losses, $\Delta P_{Cu,r}$, and iron core losses, ΔP_{Fe}:

$$\Delta P_{loss} = \Delta P_{Cu,s} + \Delta P_{Cu,r} + \Delta P_{Fe}. \tag{9}$$

where:

$$\begin{aligned}\Delta P_{Cu,s} =& \frac{3}{2} R_s \left(i_{sd}^2 + i_{sq}^2\right) = \frac{3}{2} R_s \left[\left(\frac{1}{L_m^2} + \frac{\omega_s^2}{R_{Fe}^2}\right)\psi_{md}^2 + \right. \\ & \left(\frac{1}{L_m^2} + \frac{1}{L_{\sigma r}^2} + \frac{2}{L_m L_{\sigma r}} + \frac{\omega_s^2}{R_{Fe}^2}\right)\psi_{mq}^2 + \\ & \left. \frac{2\omega_s}{R_{Fe} L_m}\psi_{md}\psi_{mq}\right],\end{aligned} \tag{10}$$

$$\Delta P_{Cu,r} = \frac{3}{2}\frac{R_r}{L_{\sigma r}^2}\psi_{mq}^2, \tag{11}$$

$$\Delta P_{Fe} = \frac{3}{2}\frac{\omega_s^2}{R_{Fe}}\left(\psi_{md}^2 + \psi_{mq}^2\right), \tag{12}$$

where R_s is the average stator resistance.

As well as for ΔP_{loss}, the electromagnetic torque T_{em} can be expressed as function of the magnetizing flux components (p is the number of pole pairs):

$$T_{em} = \frac{3}{2} p \frac{1}{L_{\sigma r}} \psi_{md}\psi_{mq} = K_T \psi_{md}\psi_{mq}. \tag{13}$$

Thus, by defining $K_T = {}^{3p}/_{(2L_{\sigma r})}$ as the torque constant, the expression of the power losses for the loss model is determined by:

$$\Delta P_{loss} = \frac{3}{2}\left(A\psi_{md}^2 + B\frac{T_{em}^2}{K_T^2\psi_{md}^2} + C\frac{T_{em}}{K_T}\right), \tag{14}$$

where

$$A = \frac{R_s}{L_m^2} + \frac{\omega_s^2}{R_{Fe}}\left(1 + \frac{R_s}{R_{Fe}}\right), \tag{15}$$

$$\begin{aligned}B =& R_s\left(\frac{1}{L_m^2} + \frac{2}{L_m L_{\sigma r}}\right) + \left(R_s + R_r\right)\frac{1}{L_{\sigma r}^2} + \\ & \frac{\omega_s^2}{R_{Fe}}\left(1 + \frac{R_s}{R_{Fe}}\right)\end{aligned} \tag{16}$$

and

$$C = \frac{2R_s\omega_s}{R_{Fe}L_m}. \tag{17}$$

In order to minimize the power losses, the optimum value of ψ_{md}, namely ψ_{md}^{opt}, is obtained by setting equal to zero the derivative of (14) with respect to ψ_{md} (the loss minimization is searched for a given stationary operating point with $T_{em} = const$):

$$\left.\frac{\partial \Delta P_{loss}}{\partial \psi_{md}}\right|_{T=const} \Longrightarrow \psi_{md}^{opt} = \sqrt{\frac{B}{A}}\left|\psi_{mq}\right|. \tag{18}$$

By considering (18) and (13), the optimum direct axis magnetizing flux component can be expressed as

$$\psi_{md}^{opt} = \sqrt{\frac{B}{A}}\left|\frac{T_{em}}{K_t\psi_{md}^{opt}}\right|, \tag{19}$$

from which it is possible to derive a formula depending on the main IM parameters and on torque:

$$\psi_{md}^{opt} = \sqrt[4]{\frac{B}{A}}\sqrt{\frac{T_{em}}{K_t}} = \sqrt[4]{\frac{B}{A}\left(\frac{T_{em}}{K_t}\right)^2}. \tag{20}$$

The optimal IM flux level depends on the synchronous speed ω_s, on the IM parameters (R_s, R_r, R_f, $L_{\sigma r}$, L_m, p) and on the applied torque T_{em}.

Unfortunately, (20) has the burden that both a square root and a 4^{th} square root must be solved simultaneously. For microcontrollers, these functions determine high computational efforts at the cost of long calculation time periods, which could bring to algorithm execution times that exceed the PWM-SVM period itself. Therefore, an alternative method for the determination of ψ_{md}^{opt} (equal to ψ_{rd}^{opt} in steady state) is presented hereinafter. It consists on a simple iterative procedure, whose algorithm is represented in the flowchart of Fig. 2. More in detail, the algorithm operates with a criterion of bisection search for the detection of the ψ_{md} value, corresponding to the minimum of power losses $\Delta P(\psi_{md})$. The first step defines the range of the search interval between a minimum and a maximum value of ψ_{md}, i.e. $\psi_{md\,min}$ and $\psi_{md\,max}$, respectively, and a search step d. Once the midpoint $x = {}^{(\psi_{md\,max}+\psi_{md\,min})}/_2$ is computed, the following conditions are applied:

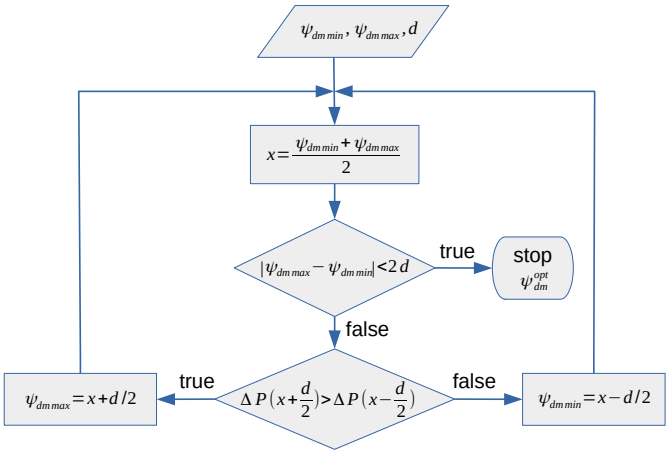

Figure 2. Flowchart of the online search algorithm.

$$\begin{cases}\psi_{md\,max} = x + \frac{d}{2} & \text{if } \Delta P(x - \frac{d}{2}) < \Delta P(x + \frac{d}{2}) \\ \psi_{md\,min} = x - \frac{d}{2} & \text{if } \Delta P(x - \frac{d}{2}) > \Delta P(x + \frac{d}{2}).\end{cases} \tag{21}$$

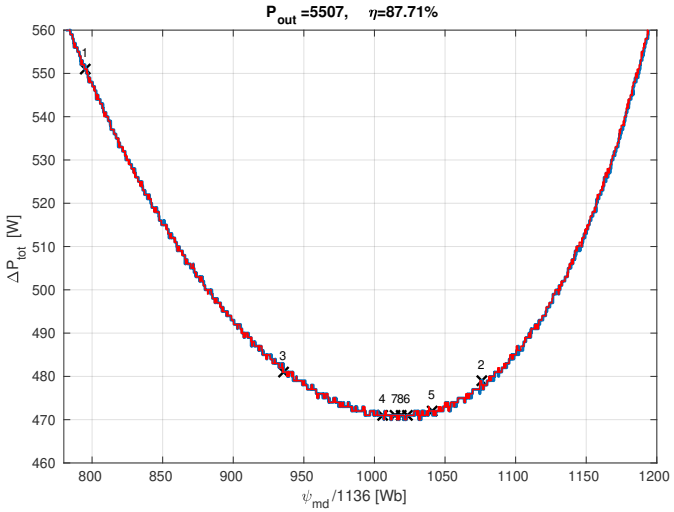

Figure 3. Calculated IM power losses and iteration process showing various steps.

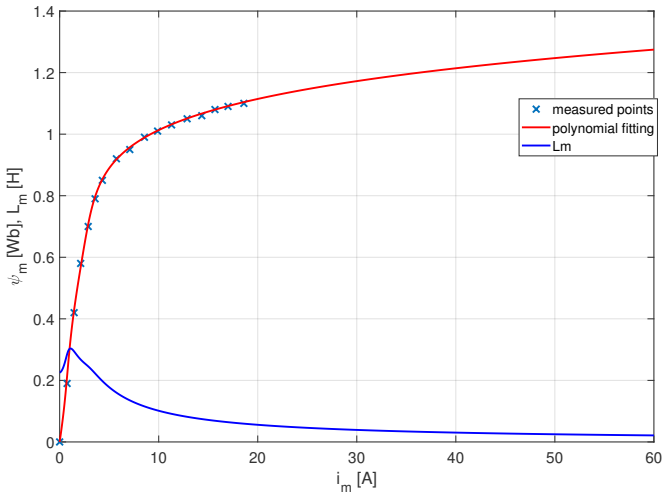

Figure 4. Magnetizing curve and trend of the magnetizing inductance L_m.

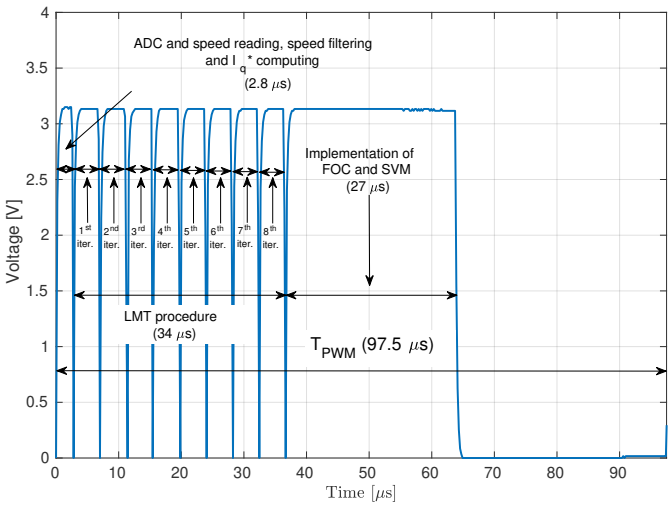

Figure 5. Timing diagram within a PWM cycle.

The iteration continues until the following condition is satisfied:

$$\Delta\psi_{md} = |\psi_{md\,max} - \psi_{md\,min}| < 2d, \tag{22}$$

which minimizes the power consumption of the electric drive.

For a more efficient implementation of the minimization procedure, a maximum number of eight iterations has been set. In this case, the algorithm converges rapidly over an initial search range of $\Delta\psi_{md} = [0.2... \ 1.2]$ Wb and a search step fixed at $d = {}^{\Delta\psi_{md}}/_{2^8} = {}^{1}/_{256} \approx 3.9 \cdot 10^{-3}$ Wb, which gives a reasonable precise solution (the search flux interval $\Delta\psi_{md}$ has been divided in about 18176 sub-intervals). The iteration process is resumed in Fig. 3, drawing attention to the minimization steps (numbered from 1 to 8), where the power losses have been calculated by applying (9) to (12) to the IM of Table I, at rated torque and rated speed; the blue curve is calculated by Matlab, whereas the red one by a ATSAM3X8E microcontroller (the search flux interval $\Delta\psi_{md}$ has been here divided in about 18176 sub-intervals). The execution time of this procedure (the 8 iterations) is about 34 μs, that of the whole FOC algorithm about 64 μs, whereas the period of each PWM cycle is about 97 μs, as shown in Fig. 5, which plots the related experimental timing diagram within a PWM period, highlighting the 8 iteration time intervals for the minimization procedure, as well as the time intervals for speed reading and filtering, direct axis current reference i^*_{sq} computing and implementation of both the FOC and SVM equations (see Fig. 6). It has to be highlighted that this minimization procedure is computed within one PWM period, in which all the electrical quantities and parameters of the IM drive are assumed as constant values, being the Space Vector Modulation (SVM) a discrete-time system working at a PWM frequency of 10253 Hz. Therefore, (9) - (21) have constant parameters within a PWM period, ensuring that only one global minimum value of ΔP can be detected.

For a more accurate model, the variation of the magnetizing reactance with saturation should be considered, instead leakage reactances are not highly affected by this phenomenon [12], [35]. Thus, the core saturation is taken into account by considering the magnetizing curve $i_m = f(\psi_m)$ depicted in Fig. 4, which has been experimentally obtained by means of a no-load test at synchronous speed. The equation that fits the related trend is given by (see Fig. 4):

$$\begin{aligned} i_m = {} & 119.6\psi_m^6 + 250.8\psi_m^5 + 181.7\psi_m^4 \\ & -44.92\psi_m^3 - 0.83\psi_m^2 + 4.43\psi_m. \end{aligned} \tag{23}$$

Moreover, for a possible implementation of (18) or (20), the nonlinear behavior of the IM can be considered conveniently by introducing the magnetizing inductance also represented in Fig. 4:

$$L_m(\psi_m) = \frac{\psi_m}{i_m(\psi_m)}. \tag{24}$$

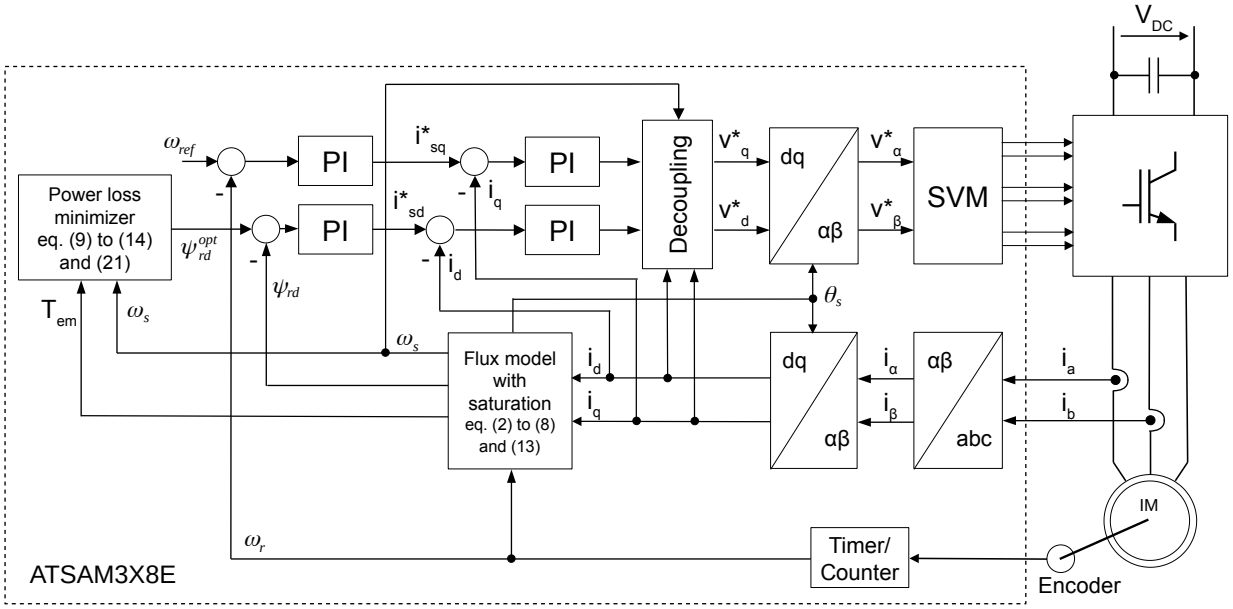

Figure 6. Block diagram for LMC implementation both in Simulink and by means of the microcontroller ATSAM3X8E.

Finally, the variability of the core loss resistance R_{Fe} is considered as a function of the frequency f and given by the following equation:

$$R_{Fe}(f) = k_0 + k_1 \cdot |f| + k_2 \cdot f^2, \tag{25}$$

where k_0, k_1 and k_2 depend on the particular type of IM and have to be identified by experimental tests. For the tested IM $k_0 = 1$, $k_1 = 2.45$ and $k_2 = 0.141$.

It must be noticed that the proposed algorithm takes into account the minimization of the controllable power losses, which depend only on the working harmonics (the other harmonic components cannot be controlled).

III. Simulation Results

The dynamic model of the induction IM, the FOC strategy and the LMT have been preliminarily implemented in the Simulink environment. According to Fig. 6, in the upper control channel, the output speed of the IM model is compared with the reference speed ω_{ref} and the error is, then, processed by a PI controller in order to provide the reference q-axis current, i^*_{sq}, which is compared with the i_{sq} current of the motor. The determined error provides the reference q-axis voltage v^*_{sq}, needed for the motor supply. The second control channel is characterized by the power loss minimizer block, which provides the optimum level of magnetization for the loss minimization, ψ^{opt}_{md}, given by the implementation of (14) and (18). The error derived from the further comparison between the reference d-axis current, i^*_{sd}, and the current of the IM, namely i_{sd}, determines the reference d-axis voltage v^*_{sd}. The performances of the simulated drive have been tested under different conditions of load and reference speed. More specifically, ω_{ref} has been varied from 50 rad/s to 300 rad/s with steps of 50 rad/s and, for each speed condition, the load torque has been varied from 0 Nm to 18 Nm with steps of 1 Nm, obtaining 114 overall conditions of operation. For each combination, the trend of the power losses ΔP_{LMT} is evaluated and compared with the losses ΔP_{FOC} computed with the traditional FOC strategy (without the adoption of LMT), working at its rated flux. Figures 7a and 7b show the comparisons between ΔP_{FOC} (blue line) and ΔP_{LMT} (green line) for ω_{ref} equal to 100 rad/s and 300 rad/s, respectively. From these simulation results, it appears clear that the adoption of the proposed LMT is more effective for low or medium loads. This aspect can be noticed by the power losses difference, namely $\Delta\Delta P$ (red line), between ΔP_{FOC} and ΔP_{LMT}.

Table I
Main rated values and parameters of the IM under test.

Quantity	Value
Power [kW]	5.5
Voltage [V]	400
Current [A]	13
Frequency [Hz]	50
Torque [Nm]	18
Rated speed [rpm]	2850
Stator resistance [Ω]	0.56
Rotor resistance [Ω]	0.77
Stator inductance [H]	0.116
Rotor inductance [H]	0.119
k_1 [$\Omega\, s$]	2.75
k_2 [$\Omega\, s^2$]	0.141
Rated rotor flux [Wb]	0.7

Other interesting results are shown in Fig.8, depicting the comparison between the trends over time of ΔP_{FOC} (blue line) and ΔP_{LMT} (red line) during an acceleration from 0 to 200 rad/s at no load conditions and with the application of its rated load at 5 s. It can be observed that, for both no load and rated load, the power loss minimizer decreases significantly the power losses involved in the machine.

Finally, the three-dimensional trend of $\Delta\Delta P$ as function of both speed and load is shown in the graph of Fig. 9. It appears

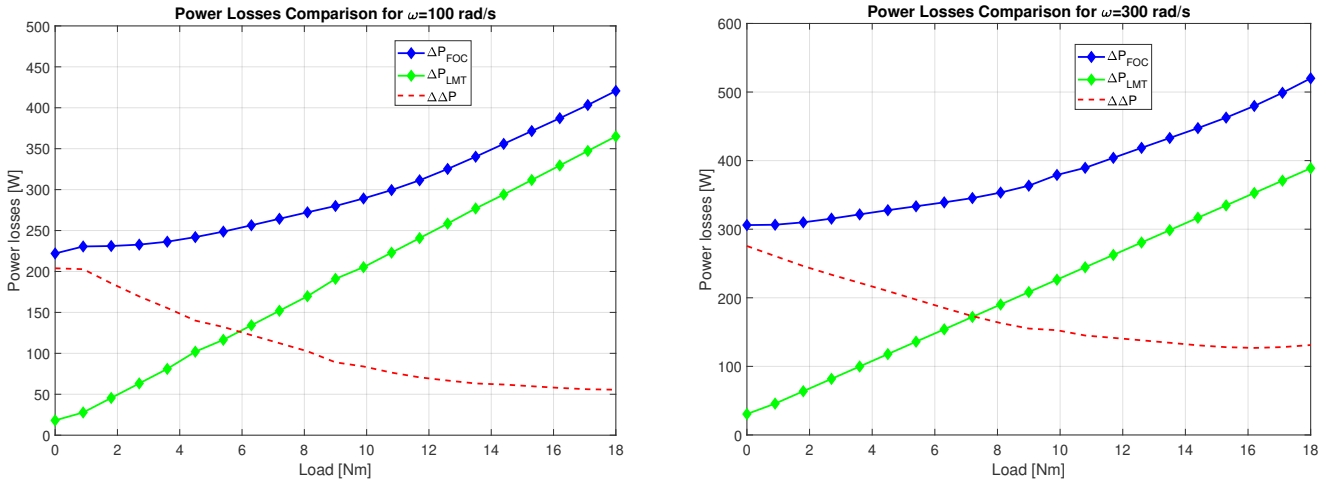

Figure 7. Comparison between the trends of the power losses between LMT and the traditional FOC for: (a) $\omega_{ref} = 100$ [rad/s] and (b) $\omega_{ref} = 300$ [rad/s].

Table II
DATA OF INVERTER SINUS-IFDE.

Parameter	Value
Input voltage [V]	380...460
Input frequency [Hz]	50/60
Input current [A]	35
Output power [kVA]	21.1
Output voltage [V]	0...380...460
Output current [A]	32
Output frequency [Hz]	0...800

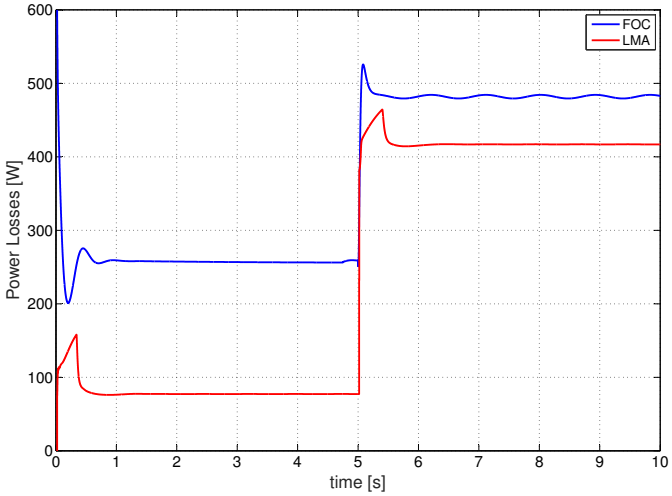

Figure 8. Comparison between the overall power losses trends between FOC (blue line) and LMT (red line).

evident that the proposed technique is much more effective for light load conditions, whereas the algorithm is not significantly affected by variations on the speed conditions.

IV. TEST BENCH EQUIPMENT AND EXPERIMENTAL RESULTS

In order to validate the simulation results described in Section III, a test bench has been set-up at EDALab (Electrical Drives Applications Laboratory - University of Palermo) and

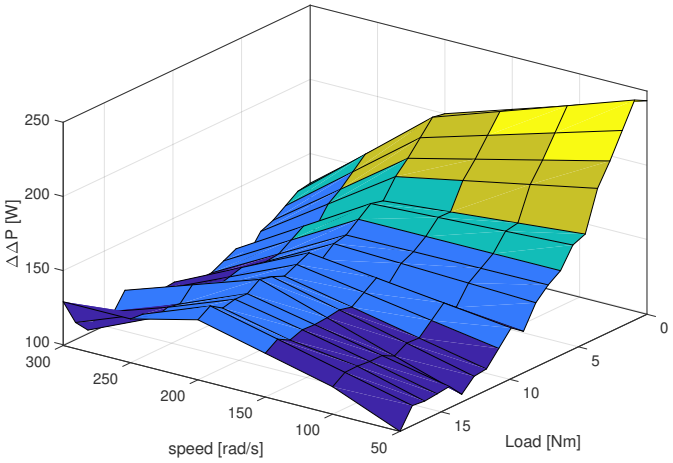

Figure 9. Three-dimensional trend of $\Delta\Delta P$ as function of the IM working conditions.

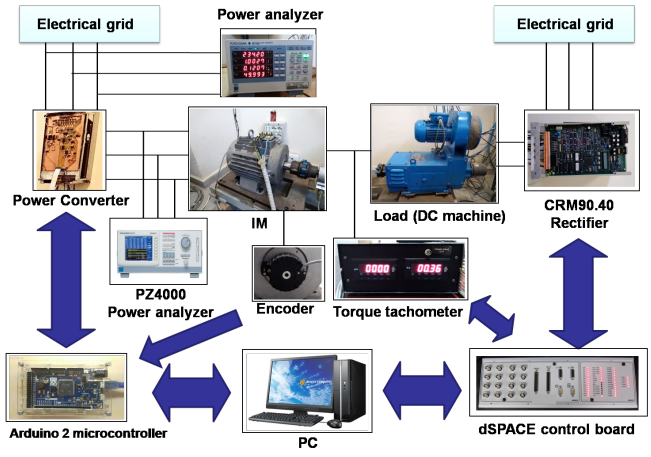

Figure 10. Schematic representation of the test bench.

Fig. 10 shows its schematic representation. The IM taken into account for the proposed analysis is a 5.5 kW three-phase machine with a double squirrel-cage rotor, whose rated values and parameters are summarized in Table I. The IM is driven by a SINUS-IFDE digital power converter (*Elettronica Santerno Inc.*), whose data are summarized in Table II and which is controlled with a SVPWM (Space Vector Pulse Width Modulation) technique with a switching frequency equal to 10.25 kHz. The motor speed is detected by an incremental encoder (Eltra Inc., model EH80) and the load is represented by a DC machine (Stipaf Elettromeccanica), with 7.83 kW of rated power and 22.5 A of rated current, driven by a CRM90.40 4-quadrant ac-dc converter (Elettronica Santerno). The FOC strategy and the LMT are experimentally implemented by means of a low-cost ATMEL ATSAM3X8E, ARM type, microcontroller, mounted on an "Arduino Due" board and running at a clock frequency of 84 MHz. The input power is measured through a PZ4000 power analyzer (Yokogawa Inc.), allowing the real-time acquisition of the rms values of both voltages and currents, whereas the output mechanical power is measured through a TT9000 torque-tachometer (Tekkal Inc.). The armature current of the DC motor is controlled by the dSPACE user interface, allowing the real-time selection of the working condition of the motor in terms of load. The speed of the IM is controlled by the Arduino Due micro-controller [36]. For each working condition, the input power and the output power are measured, both with the LMT and the FOC strategies.

In order to analyze both economic and technical aspects of the proposed implementation, the costs and performance of the adopted microcontroller are briefly compared with traditional ones. Indeed, it can be stated that systems such as DSP (Digital Signal Processor), FPGA (Field Programmable Gate Array) and CPLD (Complex Programmable Logic Device) are often used in both industrial and automotive applications; however, their high operating frequency, which clearly leads to higher performance, determines high costs. Table III economically compares the possible solutions for the implementation of the proposed control algorithm [37], [38]. As shown by this Table, it can be noticed that, at present days, the Arduino DUE is the most economic solution.

Table III
ECONOMIC ANALYSIS BETWEEN AVAILABLE MICROCONTROLLERS.

Controller	Model	Freq. MHz	Price USD
MCU	Arduino DUE (AT SAM3X8E)	84	38.00
DSP	C2000 controlCARDs-TMS320F2808	100	61.00
DSP	ADZS-BFSHUSB-EZEXT	400	112.72
DSP	TMDSCNCD28335 control card	150	69.00
DSP	TMDSPREX28335 control card	150	195.00
DSP	TMDSDOCK28069	90	109.00
FPGA+CPLD	Xilinx® Inc. EK-S6-SP605-G	1100	783.21
FPGA	Xilinx® Spartan-6 LX4 Digilent Cmod s6	133	86.00
FPGA	Xilinx® Spartan-7 Digilent Arty S7-25	50	99.00
FPGA	Zynq-7000 Xilinx® 7 Cora Z7	667	99.00
FPGA	DE0-Nano - Altera Cyclone IV	50	99.95
Max V CPLD	Intel DK-DEV-5M570ZN	247	74.90

Another advantage of the proposed Arduino DUE board is its higher flexibility, due to the easy accessibility of the interface pins. Furthermore, the lower clock frequencies (84 MHz), which are adequate for electric drive applications, avoid the thermal issues if compared to other systems [36]. The adopted microcontroller is also characterized by a high compilation and execution speed of the code implemented in C programming language, which occupies only the 5% of the memory, so that other features can be developed, such as faults management. The code is developed in the open-source Arduino IDE program, written in fixed point algebra, in order to improve the microcontroller performance. Another open source program, namely Processing, is used to create the user interface with the front control panel for data acquisition. In conclusion, it can be stated that the used microcontroller is the cheapest solution and it does not affect in a considerable manner the performance of the proposed drive.

The most significant results carried out from the experimental tests are shown in Fig. 11, which compares the trends, in terms of electrical drive input power, by applying the proposed LMT and the traditional FOC for six different values of ω_{ref}, from 50 rad/s to 300 rad/s with steps of 50 rad/s. From each graph, it can be noticed that the LMT achieves better performance with respect to the FOC, for any working condition of the IM. As a further comparison, the same Figure plots the input power trends obtained by applying the loss model proposed in [11]. As well as for the previous comparison, the proposed power loss minimizer is suitable for each of the examined working condition of the IM drive.

Moreover, Fig. 12a plots the comparison between the dynamic responses in terms of the IM angular speed obtained with the proposed minimization procedure (red line) and with the traditional FOC (blue line) during a step load change, from no load conditions to the IM rated load. It can be observed that the implementation of the power loss minimizer does not affect in a significant manner the dynamic performance of the drive except for the speed error, which appears more pronounced. This is due to the lower dynamics of the rotor flux component. For the same step change, the profiles of the three-phase currents, as well as the direct-axis and quadrature-axis stator current components, have been measured for FOC and LMT algorithms and plotted in Figs. 12b and 12c, respectively. As well as for the previous results, the trends depicted in these two Figures are comparable between each other, demonstrating the fact that the proposed algorithm provides adequate dynamic performance. Finally, the dynamic behavior of the rotor flux control loop in LMT mode is shown in Fig. 13, during a sudden speed change from 100 to 150 rad/s at t=2 s, where the optimum rotor flux reference (blue line) is compared with the feedback rotor flux (red line). Here the rotor flux tracking is guaranteed with an obvious delay that depends on the equivalent time constant of the cascaded i_d channel loops and on the rotor time constant.

The advantage of adopting the LMT can be also visualized in Fig. 14, which compares the differences in terms of power losses between the FOC strategy and the LMT for three different speed conditions (100 rad/s, 200 rad/s and 300 rad/s), by considering the following formula:

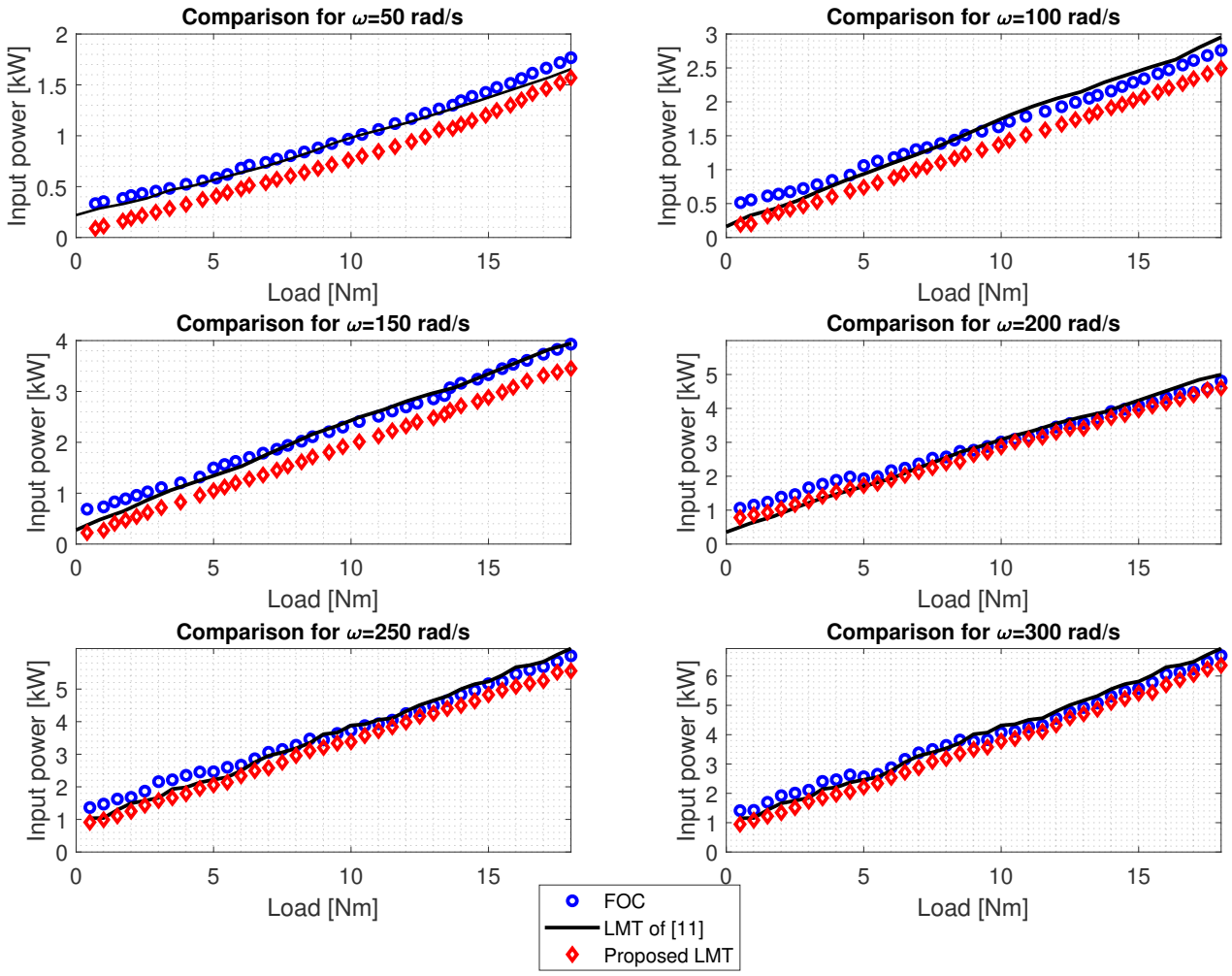

Figure 11. Comparison between the input power trends as function of the load torque with the adoption of the traditional FOC (blue color) and the proposed LMT (red color) for $\omega_{ref} = 50 \div 300$ [rad/s] with steps of 50 [rad/s].

$$\Delta\Delta P\% = \frac{P_{loss}^{FOC} - P_{loss}^{LMT}}{P_{loss}^{FOC}} \cdot 100. \tag{26}$$

From Fig. 14, it appears clear that the use of the power losses minimizer is advantageous with respect to the FOC, especially for light and medium loads. Therefore, the results demonstrate that this algorithm is suitable for a specific range of working conditions, reaching almost 15% of power loss savings for medium loads and around 10% for high loads. As evident by the figures, the power loss minimizer is less effective if the working condition is closer to the rated IM values, which is in accordance to the simulation results, as described in Section III.

V. Conclusions

In this paper, a simple and low-cost procedure for power losses minimization on a 5.5 kW IM drive has been presented. The efficiency enhancement is achieved for any condition in terms of load and speed by adequately setting in real-time the optimal value of the direct axis magnetizing flux component reducing, therefore, the power losses during the motor operation. The easy and flexible implementation of the control system is achieved by means of an ATMEL ATSAM3X8E microcontroller, which represents a good compromise between technical and economical features. The proposed LMT is firstly implemented in Simulink environment and then experimentally validated. Both the simulation and the experimental results confirm that the proposed control strategy is suitable especially for light and medium load conditions and for any value of the reference speed.

Acknowledgments

This work was financially supported by PON R&I 2015-2020 “PROpulsione e Sistemi IBridi per velivoli ad ala fissa e rotante – PROSIB”, CUP no:B66C18000290005, by Prin 2017 - Settore/Ambito di intervento: PE7 linea C - Advanced power-trains and -systems for full electric aircrafts. CUP: B74I19001480001, by SDESLab (Sustainable Development and Energy Saving Laboratory) and EDALab (Electrical Drives Applications Laboratory) of the University of Palermo.

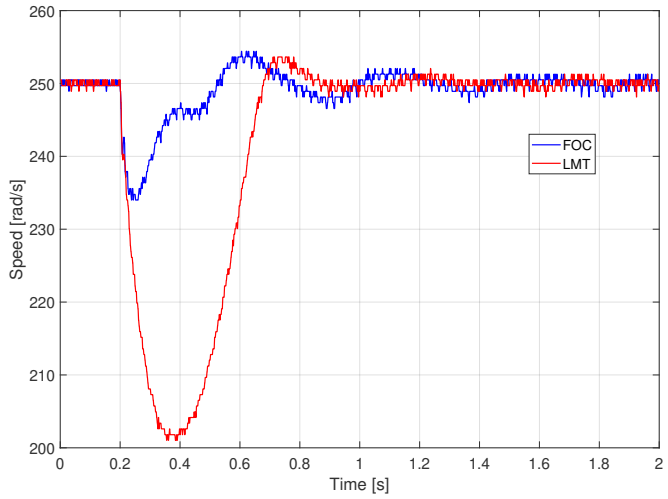

(a) Speed dynamic response comparison between traditional FOC (blue line) and LMT (red line) algorithms for a load step change from no load conditions to rated load conditions at 250 rad/s.

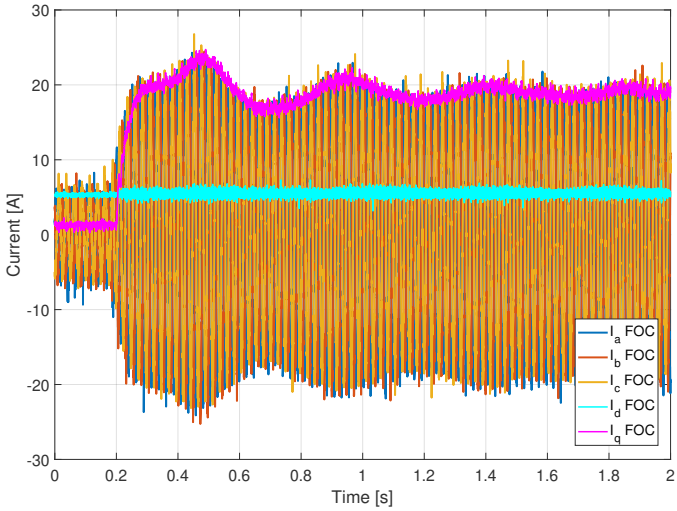

(b) Three-phase current profiles during a load step change for traditional FOC at 250 [rad/s].

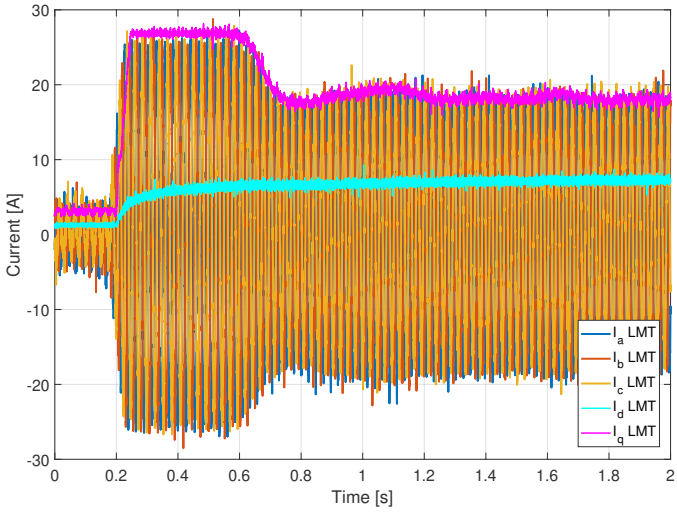

(c) Three-phase current profiles during a load step change for LMT at 250 [rad/s].

Figure 12. Dynamic performance comparison between FOC and the proposed procedure.

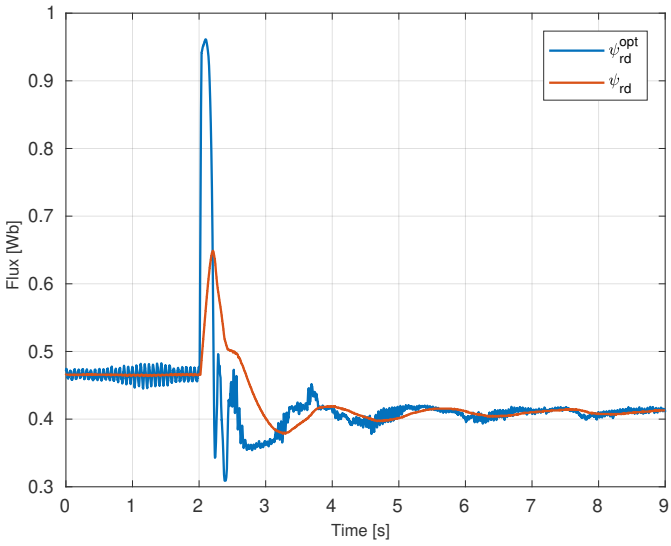

Figure 13. Dynamic response of the rotor flux control loop in LMT mode.

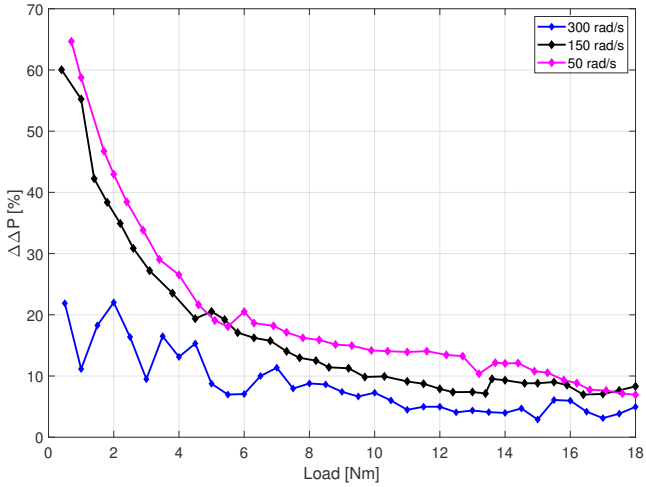

Figure 14. $\Delta\Delta P\%$ for ω_{ref}=50 rad/s (magenta line), 150 rad/s (black line) and 300 rad/s (blue line).

REFERENCES

[1] A. M. Bazzi and P. T. Krein, "Review of methods for real-time loss minimization in induction machines," *IEEE Transactions on Industry Applications*, vol. 46, pp. 2319–2328, Nov 2010.

[2] S. Kumar and K. Vasanthkumar, "Energy efficient control of three-phase induction motor," *International Journal of Computing Algorithm*, vol. 1, pp. 48–54, dec 2012.

[3] C. Chakraborty and Y. Hori, "Fast efficiency optimization techniques for the indirect vector-controlled induction motor drives," *IEEE Transactions on Industry Applications*, vol. 39, pp. 1070–1076, July 2003.

[4] F. Fernandez-Bernal, A. Garcia-Cerrada, and R. Faure, "Model-based loss minimization for dc and ac vector-controlled motors including core saturation," *IEEE Transactions on Industry Applications*, vol. 36, pp. 755–763, May 2000.

[5] S. Vaez-Zadeh and F. Hendi, "A continuous efficiency optimization controller for induction motor drives," *Energy Conversion and Management*, vol. 46, no. 5, pp. 701 – 713, 2005.

[6] F. Abrahamsen, F. Blaabjerg, J. K. Pedersen, and P. B. Thoegersen, "Efficiency-optimized control of medium-size induction motor drives," *IEEE Transactions on Industry Applications*, vol. 37, pp. 1761–1767, Nov 2001.

[7] D. S. Kirschen, D. W. Novotny, and T. A. Lipo, "Optimal efficiency control of an induction motor drive," *IEEE Transactions on Energy Conversion*, vol. EC-2, pp. 70–76, March 1987.
[8] A. Bruno, M. Caruso, A. O. Di Tommaso, C. Nevoloso, and R. Miceli, "Experimental comparison of efficiency enhancement algorithms for three-phase induction motors," in *2019 Fourteenth International Conference on Ecological Vehicles and Renewable Energies (EVER)*, pp. 1–6, May 2019.
[9] G. C. D. Sousa, B. K. Bose, and J. G. Cleland, "Fuzzy logic based on-line efficiency optimization control of an indirect vector-controlled induction motor drive," *IEEE Transactions on Industrial Electronics*, vol. 42, pp. 192–198, April 1995.
[10] G. O. Garcia, J. C. M. Luis, R. M. Stephan, and E. H. Watanabe, "An efficient controller for an adjustable speed induction motor drive," *IEEE Transactions on Industrial Electronics*, vol. 41, pp. 533–539, Oct 1994.
[11] M. N. Uddin and S. W. Nam, "New online loss-minimization-based control of an induction motor drive," *IEEE Transactions on Power Electronics*, vol. 23, pp. 926–933, March 2008.
[12] I. Kioskeridis and N. Margaris, "Loss minimization in induction motor adjustable-speed drives," *IEEE Transactions on Industrial Electronics*, vol. 43, pp. 226–231, Feb 1996.
[13] S. K. Sul and M. H. Park, "A novel technique for optimal efficiency control of a current-source inverter-fed induction motor," *IEEE Transactions on Power Electronics*, vol. 3, pp. 192–199, April 1988.
[14] J. R. Pottebaum, "Optimal characteristics of a variable-frequency centrifugal pump motor drive," *IEEE Transactions on Industry Applications*, vol. IA-20, pp. 23–31, Jan 1984.
[15] T. M. Rowan and T. A. Lipo, "A quantitative analysis of induction motor performance improvement by scr voltage control," *IEEE Transactions on Industry Applications*, vol. IA-19, pp. 545–553, July 1983.
[16] Z. Qu, M. Ranta, M. Hinkkanen, and J. Luomi, "Loss-minimizing flux level control of induction motor drives," *IEEE Transactions on Industry Applications*, vol. 48, no. 3, pp. 952–961, 2012.
[17] D. S. Kirschen, D. W. Novotny, and W. Suwanwisoot, "Minimizing induction motor losses by excitation control in variable frequency drives," *IEEE Transactions on Industry Applications*, vol. IA-20, pp. 1244–1250, Sep. 1984.
[18] B. K. Bose, N. R. Patel, and K. Rajashekara, "A neuro-fuzzy-based on-line efficiency optimization control of a stator flux-oriented direct vector-controlled induction motor drive," *IEEE Transactions on Industrial Electronics*, vol. 44, pp. 270–273, April 1997.
[19] D. S. Kirschen, D. W. Novotny, and T. A. Lipo, "On-line efficiency optimization of a variable frequency induction motor drive," *IEEE Transactions on Industry Applications*, vol. IA-21, pp. 610–616, May 1985.
[20] P. Famouri and J. J. Cathey, "Loss minimization control of an induction motor drive," *IEEE Transactions on Industry Applications*, vol. 27, pp. 32–37, Jan 1991.
[21] Gyu-Sik Kim, In-Joong Ha, and Myoung-Sam Ko, "Control of induction motors for both high dynamic performance and high power efficiency," *IEEE Transactions on Industrial Electronics*, vol. 39, pp. 323–333, Aug 1992.
[22] J. C. Moreira, T. A. Lipo, and V. Blasko, "Simple efficiency maximizer for an adjustable frequency induction motor drive," *IEEE Transactions on Industry Applications*, vol. 27, pp. 940–946, Sep. 1991.
[23] S. N. Vukosavic and E. Levi, "Robust dsp-based efficiency optimization of a variable speed induction motor drive," *IEEE Transactions on Industrial Electronics*, vol. 50, no. 3, pp. 560–570, 2003.
[24] R. Yanamshetti, S. S. Bharatkar, D. Chatterjee, and A. K. Ganguli, "A hybrid fuzzy based loss minimization technique for fast efficiency optimization for variable speed induction machine," in *2009 6th International Conference on Electrical Engineering/Electronics, Computer, Telecommunications and Information Technology*, vol. 01, pp. 318–321, 2009.
[25] A. Scarmin, C. L. Gnoatto, E. L. Aguiar, H. T. Camara, and E. G. Carati, "Hybrid adaptive efficiency control technique for energy optimization in induction motor drives," in *2010 9th IEEE/IAS International Conference on Industry Applications - INDUSCON 2010*, pp. 1–6, 2010.
[26] T. Stefanski and S. Karys, "Loss minimisation control of induction motor drive for electrical vehicle," in *Proceedings of IEEE International Symposium on Industrial Electronics*, vol. 2, pp. 952–957 vol.2, June 1996.
[27] M. H. Park and S. K. Sul, "Microprocessor-based optimal-efficiency drive of an induction motor," *IEEE Transactions on Industrial Electronics*, vol. IE-31, pp. 69–73, Feb 1984.
[28] G. Mino-Aguilar, J. M. Moreno-Eguilaz, B. Pryymak, and J. Peracaula, "An induction motor drive including a self-tuning loss-model based efficiency controller," in *2008 Twenty-Third Annual IEEE Applied Power Electronics Conference and Exposition*, pp. 1119–1125, Feb 2008.
[29] S. Sujitjorn and K. L. Areerak, "Numerical approach to loss minimization in an induction motor," *Applied Energy*, vol. 79, no. 1, pp. 87–96, 2004.
[30] R. D. Lorenz and S. . Yang, "Efficiency-optimized flux trajectories for closed-cycle operation of field-orientation induction machine drives," *IEEE Transactions on Industry Applications*, vol. 28, no. 3, pp. 574–580, 1992.
[31] Y. Shi, B. Sarlioglu, and R. D. Lorenz, "Real-time loss minimizing control of induction machines for dynamic load profiles under deadbeat-direct torque and flux control," in *2019 IEEE Energy Conversion Congress and Exposition (ECCE)*, pp. 1641–1648, 2019.
[32] Urwashi, B. Kumar, and A. Rani, "Loss minimization in induction motor drive using grey wolf optimization," in *2018 International Conference on Computing, Power and Communication Technologies (GUCON)*, pp. 770–774, 2018.
[33] A. Mannan, T. Murata, J. Tamura, and T. Tsuchiya, "Efficiency optimized speed control of field oriented induction motor including core loss," in *Proceedings of the Power Conversion Conference-Osaka 2002 (Cat. No.02TH8579)*, vol. 3, pp. 1316–1321 vol.3, April 2002.
[34] Cao-Minh Ta and Y. Hori, "Convergence improvement of efficiency-optimization control of induction motor drives," *IEEE Transactions on Industry Applications*, vol. 37, no. 6, pp. 1746–1753, 2001.
[35] I. Kioskeridis and N. Margaris, "Loss minimization in scalar-controlled induction motor drives with search controllers," *IEEE Transactions on Power Electronics*, vol. 11, pp. 213–220, March 1996.
[36] V. Castiglia, P. Ciotta, A. O. Di Tommaso, R. Miceli, and C. Nevoloso, "High performance foc for induction motors with low cost atsam3x8e microcontroller," in *2018 7th International Conference on Renewable Energy Research and Applications (ICRERA)*, pp. 1495–1500, Oct 2018.
[37] D. Luczak, "Dsp implementation of electric drive control system," in *2012 8th International Symposium on Communication Systems, Networks Digital Signal Processing (CSNDSP)*, pp. 1–3, July 2012.
[38] M. Ruba, S. Ciornei, H. Hedesiu, and C. Martis, "Complete fpga based real-time motor drive simulator with bidirectional battery and ultracapacitor power supply," in *2017 10th International Symposium on Advanced Topics in Electrical Engineering (ATEE)*, pp. 186–191, March 2017.

Adriana Bruno was born in Palermo (Italy) on 29 October 1992, studied at the University of Palermo where she graduated in Electrical Engineering in March 2019 with a thesis on loss minimization techniques in induction motors. In May of the same year she started working for Schneider Electric Industrie Italia SpA in Stezzano as a plant project manager for medium voltage switchgear for secondary electrical distribution. Since July 2020 she is the quality specialist for the MV switchgear and circuit breaker manufactoring lines.

Massimo Caruso received the M.S. and Ph.D. degrees in electrical engineering from the University of Palermo, Italy, in 2008 and 2012, respectively. In 2011, he joined the MEMS Sensors and Actuators Laboratory Group, University of Maryland, College Park, MD, USA, collaborating for the development of electric micromotors and drives for in vivo bacteria biofilm detection and treatment. In 2014, he joined the Sustainable Development and Energy Saving Laboratory, University of Palermo, Italy, focusing his research activities on the design, simulation and experimental development of electrical machines and drives for industrial and sustainable energy applications.

Antonino Oscar Di Tommaso was born in Tübingen, Germany, on June 5, 1972. He received the Master's and Ph.D. degrees in electrical engineering from the University of Palermo, Italy, in 1999 and 2004, respectively. He was a Post Ph.D. Fellow of Electrical Machines and Drives with the Department of Electrical Engineering, University of Palermo, from 2004 to 2006 and researcher from 2006 to 2019. He is currently Associate Professor of Electrical Machines and drives with the Department of Engineering (DIING), University of Palermo. His research interests include electrical machines, drives, diagnostics on power converters, and diagnostics and design of electrical machines.

Rosario Miceli Rosario Miceli (M'01) received the B.S. degree in electrical engineering and the Ph.D. degree from the University of Palermo, Palermo, Italy, in 1982 and 1987, respectively. He is a Full Professor of electrical machines with the Polytechnic School, University of Palermo. He is a Personnel in Charge of the Sustainable Development and Energy Savings Laboratory of the University of Palermo. His main research interests include mathematical models of electrical machines, drive system control, and diagnostics, renewable energies, and energy management. Dr. Miceli is a Reviewer for the IEEE Transactions on Industrial Electronics and the IEEE Transactions on Industry Applications.

Claudio Nevoloso received the M.S. and Ph.D. degrees in electrical engineering from the University of Palermo, Palermo, Italy, in 2016 and 2020, respectively. He is actually a postdoctoral researcher of SDESLAB (Sustainable Development and Energy Saving Laboratory) of University of Palermo. His main research fields involve the design, mathematical modelling and characterization of electrical machines and drives.

Fabio Viola received the M.Sc. and Ph.D. degrees in electrical engineering from the Universit'a degli Studi di Palermo, Palermo, Italy, in 2002 and 2006, respectively. In 2008, he joined the Department of Electrical, Electronic, and Telecommunication Engineering, University of Palermo, Palermo, as a Researcher. Since the same year, he holds the basic electrical engineering course. His research interests include the field of electromagnetic compatibility, high voltage, partial discharges diagnosis, renewable energy, electric vehicles, power electronic converters and energy harvesting.